ISSN 1573-160X, *PHYSICAL OCEANOGRAPHY*, Vol. 31, Iss. 3, pp. 364-386 (2024)
Original Russian Text © A. V. Smirnov, V. V. Ivanov, A. A. Sokolov, 2024,
published in *Morskoy Gidrofizicheskiy Zhurnal*, 2024, Vol. 40, Iss. 3, pp. 402–425

Original article

Comparison Analysis of Heat and Mass Transport through Fram Strait Calculated Using the Mooring and Ocean Reanalysis Data

A. V. Smirnov [1, ✉], V. V. Ivanov [1, 2], A. A. Sokolov [1]

[1] *Arctic and Antarctic Research Institute, Saint Petersburg, Russian Federation*
[2] *M. V. Lomonosov Moscow State University, Moscow, Russian Federation*
✉ *avsmir@aari.ru*

Abstract
Purpose. This paper presents a comparison analysis of water, heat and salt transports through Fram Strait calculated by using mooring and GLORYS2v4, ORAS5, GloSea5 and C-GLORSv7 reanalyses data.
Methods and Results. Mooring data were interpolated into a regular grid with the resolutions of 0.25° over longitude and 10 m over depth using the Ordinary Kriging. Unified algorithms for both mooring and reanalysis data were applied to calculate the transports for 1997–2018 in Fram Strait (8°W, 8°E). The mooring and reanalysis time series were compared, and the results were visualized.
Conclusions. It is shown that the ensemble of reanalyses in general underestimates the transports calculated by using the observation data, by 25%. The best agreement between the results obtained from reanalyses and the observation data is obtained for the West Spitsbergen Current core which is well covered by the observation data. It is revealed that the ensemble of models describes the observation data variability the best, and the FOAM and CGLO reanalyses – the greater part of temporal variability of the flows calculated by the mooring data. The data consistency in the winter period (October – March) is shown to be higher than that in the summer one (April – September). That can be related both to the reanalysis imperfections (ice melt accounting) and the season, namely summer, when moorings are usually replaced, which can result in additional errors in combining the time series.

Keywords: Arctic Ocean, Fram Strait, current, water masses, heat and mass transport, moorings, direct measurements, reanalysis

Acknowledgments: The study was carried out with support of the Russian Science Foundation grant № 24-17-00041. The work by A. A. Sokolov was supported by the Russian Science Foundation grant № 24-27-00221.

For citation: Smirnov, A.V., Ivanov, V.V. and Sokolov, A.A., 2024. Comparison Analysis of Heat and Mass Transport through Fram Strait Calculated Using the Mooring and Ocean Reanalysis Data. *Physical Oceanography*, 31(3), pp. 364-386.

Introduction

Information about the state of the ocean in modern oceanological research can be obtained using instrumental measurements, numerical modeling, and their combination – reanalysis. Remote and satellite observations allow to monitor the ocean surface and ice cover state, but do not extend to the entire water column, where significant hydrophysical processes develop. Contact observations in modern oceanography include primarily CTD (Conductivity Temperature Depth) soundings, current velocity measurements with an acoustic Doppler profiler (ADCP), data from autonomous moored [1] and drifting profiling buoys (ARGO [2], ITP [3]). Based on the measurement data of thermohaline characteristics, it is possible to calculate relative water transport rates along hydrological sections. The use of data from satellite altimeters and scatterometers allows to reduce relative water transport rates to absolute ones [1, 2]. If measurements are carried out on spatially close sections, these data can be used to study changes in ocean characteristics and determine trends in changes for individual regions or the ocean as a whole [3]. Ocean reanalyses obtained through observational data assimilation in numerical models have recently become an alternative source of information for studying hydrophysical structure of waters and their spatiotemporal variability [4, 5]. Hydrophysical parameters simulated in numerical models and reanalysis products, as a rule, differ from instrumental measurement data, which predetermines the need for an objective estimate of calculation quality by comparison with the data from direct measurements in the ocean.

The present paper studied the Fram Strait, which is the widest deep-sea strait connecting the North European Basin (NEB) with the Arctic Basin (AB) of the Arctic Ocean (AO) [6]. Through the eastern part of the Fram Strait with the West Spitsbergen Current, warm salty waters of Atlantic origin enter the AB, which are commonly called Atlantic waters (AW) [7], and through the western part of the strait, cold surface Arctic waters and cooled desalinated intermediate waters are transported to the NEB. The processes of heat and mass transport through the Fram Strait, primarily associated with AW, the main advective heat source for AB [8], have always been the focus of polar oceanographic research [9–11]. According to the existing historical estimates, the AW flux through the Fram Strait varies within very wide limits: from 1.4 to 7.1 Sv [12]. In this case, a significant part of the dispersion accounts for short-period intra-annual variability [13]. Detailed instrumental measurements of current velocity on a repeating section along 79°N started in 1997 and continuing to the present day within the ASOF international project (Arctic and Subarctic Ocean Fluxes) confirmed Ogard's hypothesis and showed that the total average annual flux in the West Spitsbergen Current is within 6.6 ± 0.4 Sv and the AW flux share (with a temperature over 2 °C) accounts for only 3.0 ± 0.2 Sv and the rest is the share of seasonally varying eddy transport [11].

The aim of the present paper was a quantitative comparison of heat and mass transport processes calculated from long-term instrumental measurements in the Fram Strait within the ASOF project framework with the products of ocean reanalyses. The relevance of such a comparison is due to the widespread use of ocean reanalyses to study the hydrophysical structure of the World Ocean waters, including the AO [14–16], in the virtual absence of objective criteria to judge how adequately the parameters of large-scale transport in the ocean simulated in reanalyses correspond to those observed in real life. The paper presents the results of a comparative analysis of volume, heat and salt fluxes calculated from instrumental observations at moorings in the Fram Strait with similar fluxes calculated from the GLORYS2v4, ORAS5, GloSea5 and C-GLORSv7 reanalyses.

[1] Nansen and Amundsen Basins Observational System. *NABOS*. [online] Available at: https://uaf-iarc.org/nabos/ [Accessed: 03 June 2024].

[2] *ARGO*. [online] Available at: http://www.argo.ucsd.edu/ [Accessed: 03 June 2024].

[3] Woods Hole Oceanographic Institution. *Ice Tethered Profilers*. [online] Available at: https://www2.whoi.edu/site/itp/ [Accessed: 03 June 2024].

Research data and methods

The study used data from instrumental observations in the Fram Strait carried out as part of the ASOF international project (available at: https://asof.awi.de/science/projects/13-monitoring-of-oceanic-fluxes-across-fram-strait/) by scientists from the Alfred Wegener Institute, Germany (AWI) and the Norwegian Polar Institute (NPI). AWI moorings cover the eastern part of the strait, while NPI moorings provide monitoring of its western part (Fig. 1).

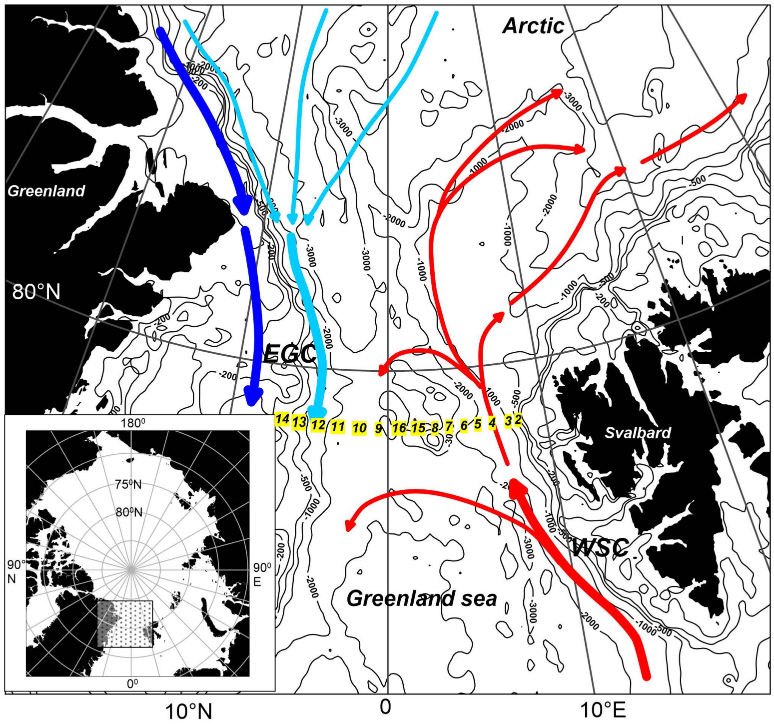

F i g. 1. Spatial positions of moorings (numbers against a yellow background) selected for analysis. Red curves show the West Spitsbergen current (WSC), blue curves – the East Greenland coastal current, and light blue ones – the East Greenland current (EGC)

Both institutes started the Fram Strait monitoring in 1997 and continue to this day. Over the past period, the position of the moorings has changed: some were excluded from the observation network, some were added, some changed their location. To measure temperature and conductivity, SBE 37 with a measurement accuracy of 0.1% pressure, 0.001 °C temperature and 0.001 S/m conductivity was used (available at: www.seabird.com). Current velocity was measured using RCM-7, RCM-9 (with an accuracy of 0.01 m/s) and ADCP 300 KHz (with an accuracy of 0.01 m/s).

Instrumental observations of AWI

AWI measurement data are presented at PANAGEA (available at: www.pangaea.de), which contains two generalizing data sets: 1997–2016 [4] and

[4] Von Appen, W.-J., Beszczynska-Möller, A., Schauer, U. and Fahrbach, E., 2019. *Physical Oceanography and Current Meter Data from Moorings F1-F14 and F15/F16 in the Fram Strait, 1997-2016* [dataset bibliography]. PANGAEA. https://doi.org/10.1594/PANGAEA.900883

2016–2018 [5]. Collectively, data from 171 moorings were selected and downloaded from September 1997 to June 2018.

Most moored buoys were positioned to obtain long continuous series of observations. Such time series had the same name (*F1–F10*), although their coordinates differed somewhat from year to year. The downloaded initial data underwent additional processing, which included formatting, grouping by parameters (separately for temperature, electrical conductivity, and current velocity components) and by time. For each day, all available values for a given parameter were selected and recorded in files in the form "latitude, longitude, depth, value". The values within one day were averaged so that the data discreteness was consistent with the reanalyses data discreteness.

Although the initial data were quality controlled [17], the time series analysis indicated that additional procedures were required. It was revealed that six time series had negative measurement horizons. Such data were rejected. Additionally, the data beyond the boundaries of physical variability were filtered out. The criteria below were selected based on statistical analysis of the original data. The data beyond 3σ were excluded from the analysis. Thus, for temperature the range would be −2.5÷6 °C, for salinity 30÷36 PSU. The current velocity components were filtered out if the velocity exceeded 2 m/s. The longest time series with moorings located at 78.5°N were selected from the processed data array (Fig. 1). The criterion for selecting measurement data of a particular mooring for subsequent analysis was the duration of the time series and spatial position, which allows the data to be used to construct a vertical section through the Fram Strait.

F1 mooring data were not used due to the short time series, while the *F15* and *F16* mooring series, which also produced relatively short time series, were retained as they were located inside the section and, due to this, allowed to improve spatial interpolation results. The final composition of AWI mooring included in the analysis is given in Table 1.

T a b l e 1

Mooring metadata

Autonomous buoy station	Longitude, °E	Time periods	Autonomous buoy station	Longitude, °E	Time periods
F1	8.6	1997–2009	*F16*	0.4	2002–2014
F2	8.3	1997–2018	*F9*	−0.4	1997–2016
F3	8.0	1997–2018	*F10*	−2.0	1997–2016
F4	7.0	1997–2018	*F11*	−3.0	1997–2015
F5	6.0	1997–2018	*F12*	−4.0	1998–2015
F6	5.0	1997–2016	*F13*	−5.0	1997–2015
F7	4.0	1997–2015	*F14*	−6.5	1997–2015
F8	2.7	1997–2014	*F17*	−8.0	2003–2015
F15	1.6	2002–2014			

[5] Von Appen, W.-J., 2019. *Physical Oceanography and Current Meter Data (Including Raw Data) from FRAM Moorings in the Fram Strait, 2016-2018* [dataset bibliography]. PANGAEA. https://doi.org/10.1594/PANGAEA.904565

Instrumental observations of NPI

The data from the NPI moorings are available at https://www.npolar.no/en/. Two data sets were downloaded: 1997–2009 [6] and 2009–2015 [7]. The downloaded data were converted into a format like that used for the AWI data. The quality control described in the previous subsection was applied to the NPI data. Values outside physical variability boundaries were filtered out, as well as erroneous data and metadata found in the analysis of the original time series. Figure 1 shows the spatial location of NPI moorings, their metadata are shown in Table 1.

F17 mooring was excluded from further analysis due to its insufficiently long time series. *F11–F14* moorings changed their position in 2002 from 79°N to 78.5°N to match the position of the AWI buoys.

The processed arrays of AWI and NPI instrumental observations were combined into a single array to obtain the best spatial coverage of the Fram Strait. According to the method [10], monthly data averaging was used. The total time coverage of the single dataset was 217 months (August 1997 – August 2015).

Reanalyses data

Instrumental observations at moorings today are probably one of the most reliable sources of information on the temporal variability of the vertical hydrophysical structure of the World Ocean waters. However, due to objective reasons, the amount of instrumental data is limited in time and space, which requires the use of alternative sources of information. They include ocean reanalysis products obtained by synthesizing observations and mathematical modeling [18] and allowing a significantly more detailed structure and water dynamics simulation.

In the present paper Global Ocean Ensemble Physics Reanalysis [8] developed by Copernicus Marine Environment Monitoring Service (CMEMS) is used. It is a compilation of four ocean reanalyses:

– GLORYS2V4 (Mercator Ocean, France),
– ORAS5 (ECMWF, EU),
– GloSea5 (Met Office, Great Britain),
– C-GLORSv7 (CMCC, Italy).

Global Ocean Ensemble Physics Reanalysis (further – CMEMS Reanalysis) data presented on a regular grid for the entire World Ocean with a spatial step of 0.25° in latitude and longitude and a time resolution of 1 day. Now, the time range of the array is 27 years (from January 1993 to December 2019). In this study, the values of the following parameters were used: potential temperature, °C; practical salinity, PSU; current velocity components directed to the north (u) and east (v), m/s. Monthly, seasonal and annual averages were calculated using daily data. Seasonal averaging was carried out over two periods for each year: winter (October – March) and summer (April – September). The CMEMS reanalysis grid (0.25°)

---

[6] De Steur, L., 2019. *Moored Current Meter Data from the Western Fram Strait 1997-2009* [data set]. Norwegian Polar Institute. https://doi.org/10.21334/npolar.2019.8bb85388

[7] De Steur, L., 2021. *Moored Current Meter and Hydrographic Data from the Fram Strait Arctic Outflow Observatory since 2009* [data set]. Norwegian Polar Institute. https://doi.org/10.21334/npolar.2021.c4d80b64

[8] Copernicus Marine Service Information (CMEMS). Marine Data Store (MDS). *GLOBAL_MULTIYEAR_PHY_ENS_001_031: Global Ocean Ensemble Physics Reanalysis*. doi:10.48670/moi-00024 [Accessed: 04 June 2024].

permits to avoid additional spatial interpolation. Since the algorithm for calculating the integral transport of volume, heat, and mass (see next section) does not require additional re-interpolation of values to standard horizons, the vertical horizons in the reanalysis grid were not recalculated into the calculation grid.

Spatial interpolation

To carry out the calculation of heat and mass transport processes and subsequent comparative analysis, the initial data of the combined array of instrumental observations were interpolated into regular grid nodes (in the format of a vertical section with a fixed step in depth and longitude) (Fig. 2).

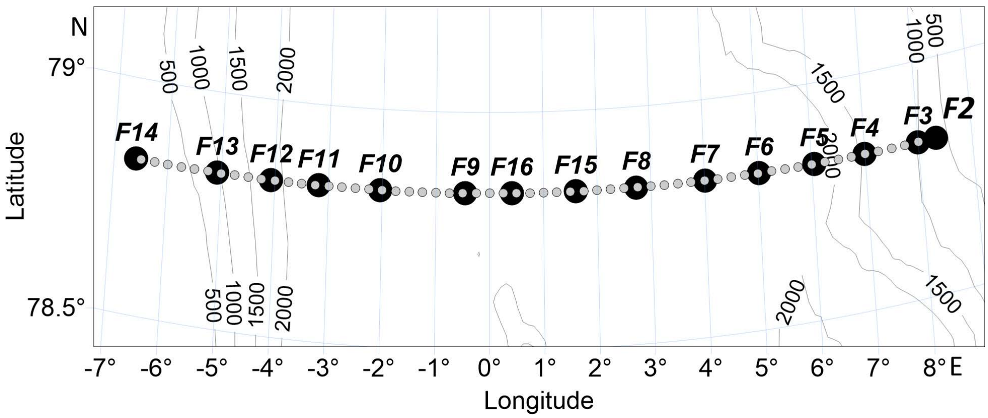

F i g. 2. Geographical location of moorings and regular grid nodes, where spatial interpolation was carried out

Ordinary kriging was chosen as an interpolation method [19]. The term "kriging" refers to a family of linear spatial regression algorithms. The use of kriging methods permits to carry out an interpolation procedure with data that have a few specific features, such as spatial heterogeneity, significant anisotropy, and presence of trends in the data [20]. The Surfer package (available at: https://www.goldensoftware.com/) was chosen as a software implementation of the kriging method.

All 217 data files for each month were restored to grid nodes, the horizontal step of which was 0.25° (6.5°W – 8°E), while the data on the vertical axis were interpolated with a step of 10 m. For further use, the interpolation results were converted into the net CDF format, which allowed to apply a unified program code for subsequent calculations. At the *in situ* conversion stage, the water temperature was converted to potential. Practical salinity and current velocity remained unchanged. By analogy with the reanalysis data, the obtained interpolated measurement data on the moorings were averaged by season (April – September and October – March) and by year.

Figure 3 shows the annual values of meridional current velocities according to the mooring data (Fig. 3, *a*) and reanalysis (Fig. 3, *b*).

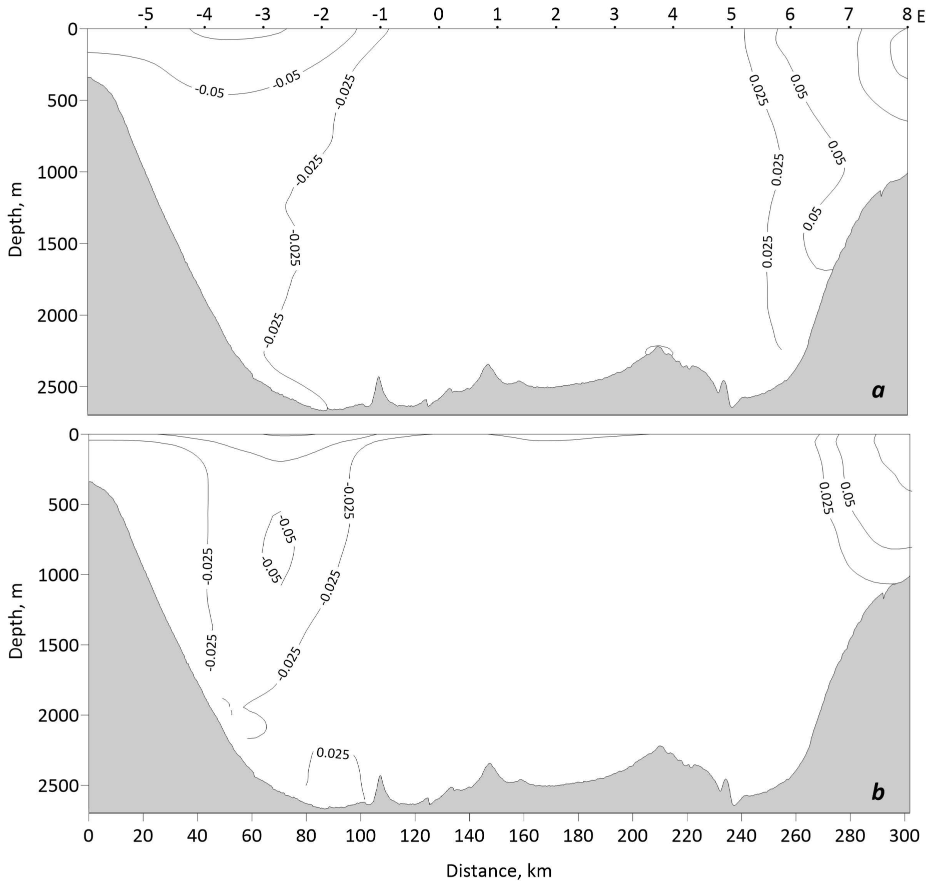

F i g. 3. Annual average values of current meridional velocities based on the mooring (*a*) and reanalysis (*b*) data

Calculation of total transport of water, heat and salt

The total transport of volume, heat and salt through the section was chosen as the main characteristic for comparison of measured time series and CMEMS reanalyses data. The total water transport (D_w) represents the integral volume transport in each depth range through a unit segment corresponding to a section node. The integral D_w along the entire length of the section determines the total volume transport through the entire section in the direction normal to the section axis. For the Fram Strait, the following statement is true:

$$Vn = v_0, \quad (1)$$

where Vn is current velocity normal to the section axis; v_0 is northward component of current velocity.

For each node of the section, $Vn(z)$ was integrated vertically to obtain the total water transport D_W ($\mathrm{m}^2 \cdot \mathrm{s}^{-1}$):

$$D_\mathrm{W} = \int_{z_l}^{z_\mathrm{up}} Vn(z) \approx \sum_j 0{,}5(Vn_j + Vn_{j+1})(z_{j+1} - z_j)\,,\ z_l \le z_j \le z_\mathrm{up}. \quad (2)$$

Product of temperature anomaly ($T(z) - T_{ref}$) and current velocity proportional to heat flux (D_H, W · m^{-1}):

$$D_H = \int_{z_l}^{z_{up}} \rho c_p Vn(z)(T(z) - T_{ref})dz \approx$$

$$\approx \sum_j 0.5\rho c_p\left[Vn(T_j - T_{ref}) + Vn(T_{j+1} - T_{ref})\right](z_{j+1} - z_j), \quad z_l \le z_j \le z_{up}. \quad (3)$$

The product of salinity anomaly ($S(z) - S_{ref}$) and current velocity is proportional to the salt flux (D_S, kg·m^{-1}·s^{-1}):

$$D_S = \int_{z_l}^{z_{up}} \rho Vn(z)(S(z) - S_{ref})dz \approx$$

$$\approx \sum_j 0.5\rho\left[Vn_j(S_j - S_{ref}) + Vn_{j+1}(S_{j+1} - S_{ref})\right](z_{j+1} - z_j), \; z_l \le z_j \le z_{up}. \quad (4)$$

In formulas (2)–(4), z_l and z_{up} are the lower and upper integration limits; c_p is specific heat capacity of sea water at constant pressure; ρ is sea water density (c_p and ρ were calculated using the *TEOS*-10 equation of state); Vn_j is current velocity at z_j level; T_j and S_j are temperature and salinity measured at z_j level, T_{ref} = –1.8°C, S_{ref} = 0, respectively.

The total transport values (F_W, F_H and F_S) were calculated by horizontally integrating the depth-averaged fluxes along the entire length of the section (L). The following formulas (5)–(7) were used:

$$F_W = \int_{(L)} D_W dl \approx \sum_{i=1}^{5} 0.5(D_{W_i} + D_{W_{i+1}})\Delta l_{i,i+1}, \quad (5)$$

$$F_H = \int_{(L)} D_H dl \approx \sum_{i=1}^{5} 0.5(D_{H_i} + D_{H_{i+1}})\Delta l_{i,i+1}, \quad (6)$$

$$F_S = \int_{(L)} D_S dl \approx \sum_{i=1}^{5} 0.5(D_{S_i} + D_{S_{i+1}})\Delta l_{i,i+1}, \quad (7)$$

where i is section node number relative to its beginning; $\Delta l_{i,\,i+1}$ is distance between two adjacent nodes, indicated as i and $i + 1$.

It should be noted that the algorithm above was modified for the reanalysis data. For example, in the NEMO model that underlies the GLOR, ORAS and CGLO reanalyses, density is not a function of temperature and salinity. Therefore, in formulas (3)–(4), the c_p and ρ quantities were taken as constants (c_p = 3989.24495292815 J/(kg·K), ρ = 1035 kg/m^3).

The above method for calculating heat and mass transport was implemented in the *Julia* language. The data from instrumental observations and reanalyses were processed by the same program code. The calculation results are presented in the next section.

Results and their discussion

Total heat and mass transport through the Fram Strait

A comparative analysis of instrumental observation and reanalysis data started with monthly data. Figures 4–6 show time series of volume, heat and salt transport through the Fram Strait for various averaging periods in 1997–2015. The monthly series were smoothed with a moving average over an 11-month window and seasonal and annual data were left unchanged. Integrated values were calculated for the entire section (6.5°W – 8°E) and throughout the entire water column.

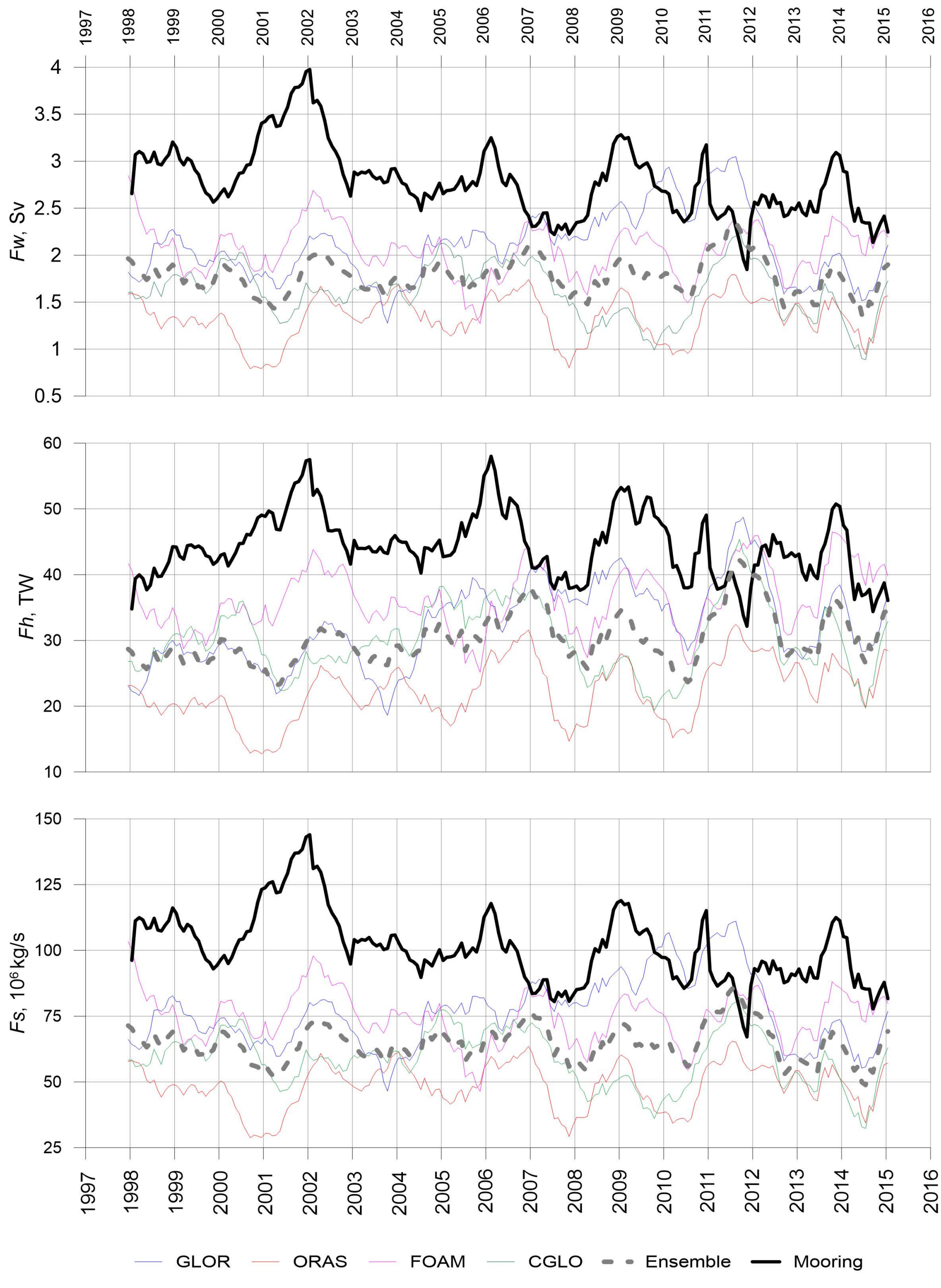

F i g. 4. Time series of heat and mass transport through the Fram Strait calculated by monthly average data

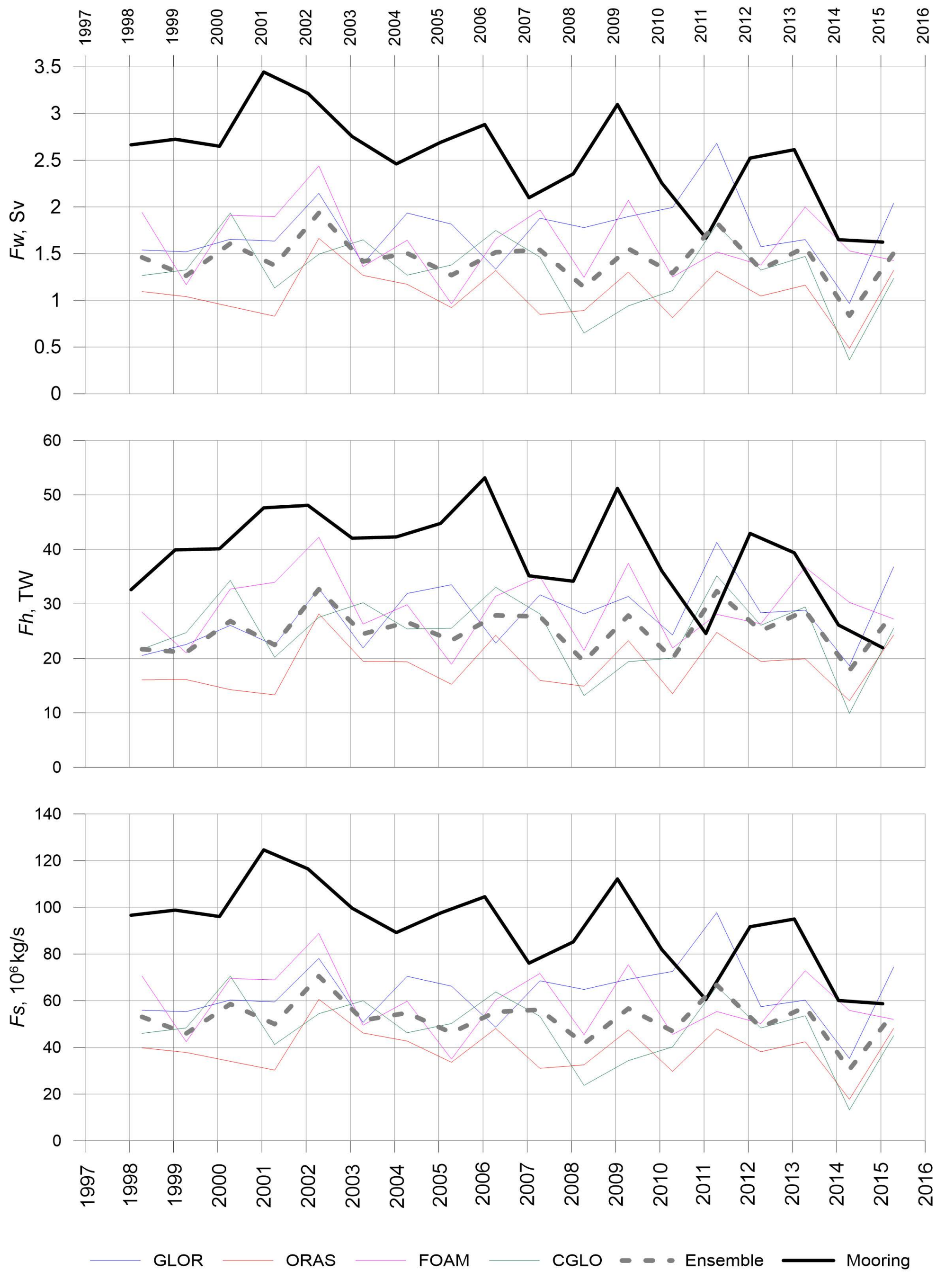

F i g. 5. Time series of heat and mass transport through the Fram Strait calculated by seasonal (April – September) average data

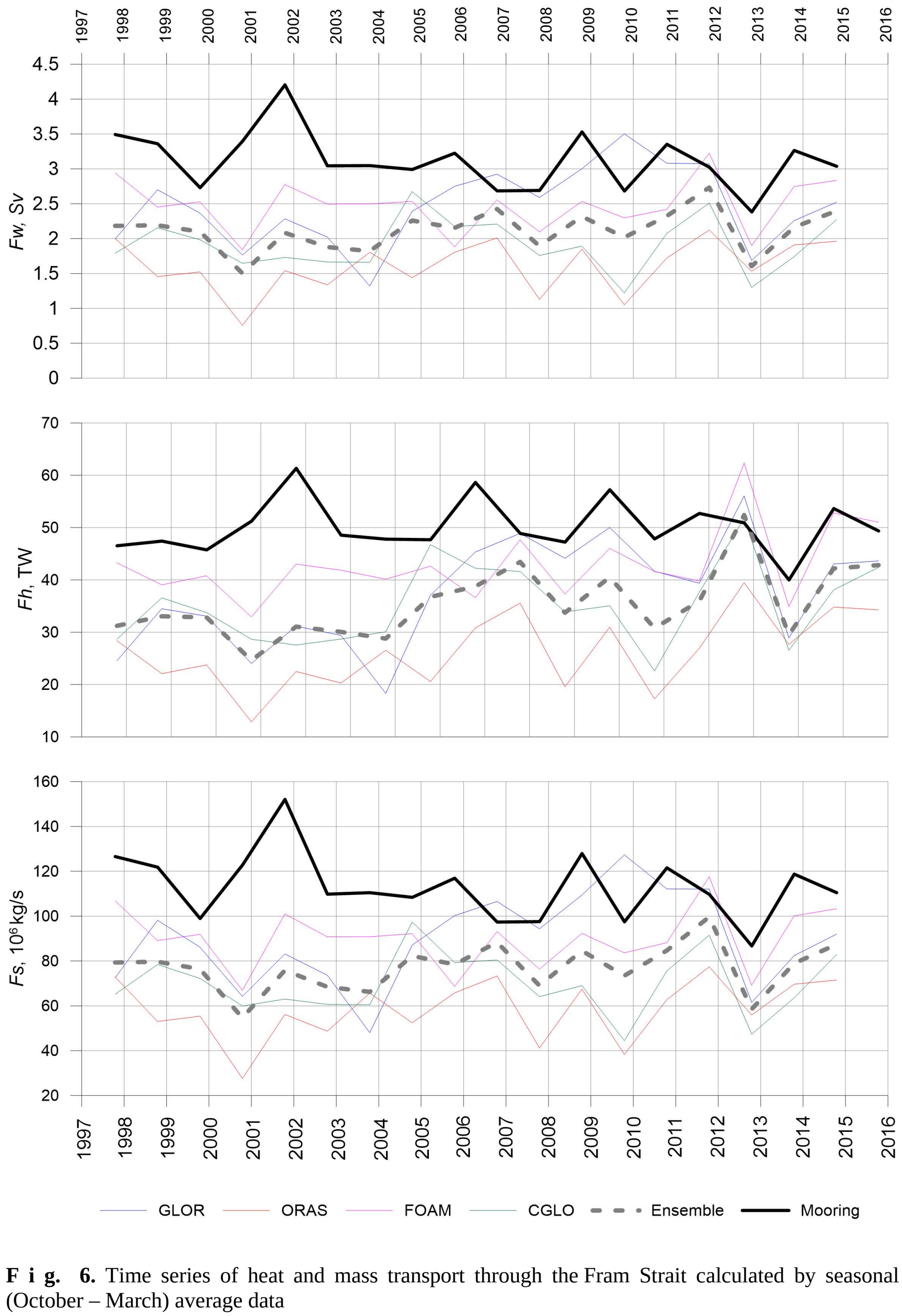

F i g. 6. Time series of heat and mass transport through the Fram Strait calculated by seasonal (October – March) average data

Figure 4 shows that the reanalysis data generally underestimate heat and mass transport value. Thus, the average value of volume transport, according to the mooring data, is higher than the ensemble average by more than 30% and its standard deviation is 50% higher. A similar picture is observed in heat and salt transport (Table 2).

Seasonal time series (Figs. 5–6) show that reanalyses underestimate heat and mass transport in summer, while better consistency is observed in winter. Annual averaging logically occupies an intermediate position (Fig. 7).

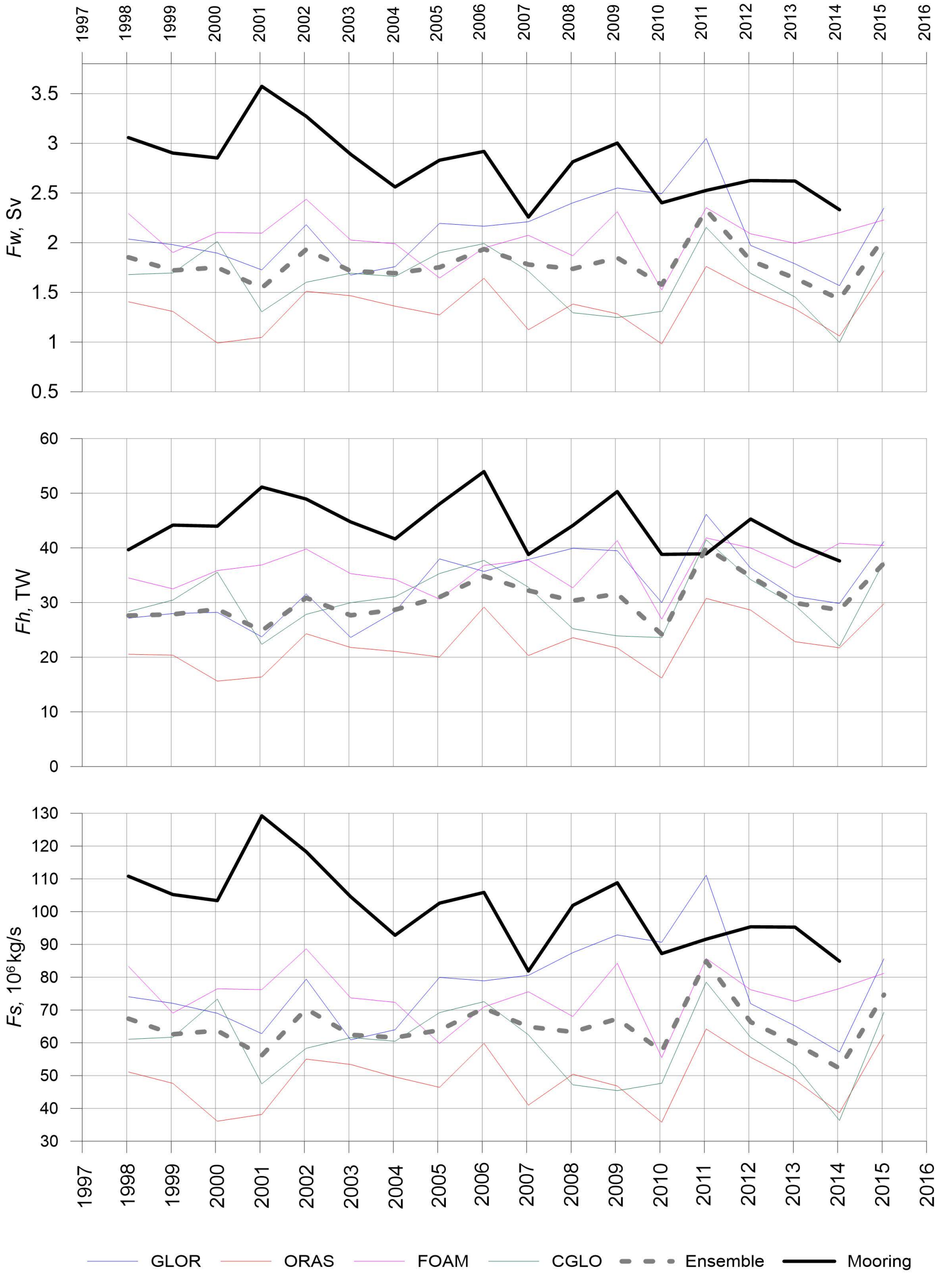

F i g. 7. Time series of heat and mass transport through the Fram Strait calculated by annual average data

Table 2

Basic statistical characteristics of the studied monthly series of data

Parameter	GLOR	ORAS	FOAM	CGLO	Ensemble	Mooring
			Fw			
Minimum	1.57	0.98	1.53	1.00	1.43	2.26
Maximum	3.05	1.76	2.44	2.15	2.33	3.57
Average	2.11	1.34	2.05	1.63	1.78	2.79
Standard deviation	0.37	0.24	0.23	0.31	0.20	0.34
Dispersion	0.14	0.06	0.05	0.10	0.04	0.12
			Fh			
Minimum	24.0	16.0	27.0	22.0	24.0	38.0
Maximum	46.0	31.0	42.0	42.0	40.0	54.0
Average	33.0	22.0	36.0	30.0	31.0	44.0
Standard deviation	6.0	5.0	4.0	6.0	4.0	5.0
Dispersion	36.0	25.0	16.0	36.0	16.0	25.0
			Fs			
Minimum	57.0	36.0	56.0	36.0	52.0	82.0
Maximum	111.0	64.0	89.0	79.0	85.0	129.0
Average	77.0	49.0	75.0	59.0	65.0	101.0
Standard deviation	14.0	9.0	8.0	11.0	7.0	12.0
Dispersion	196.0	81.0	64.0	121.0	49.0	144.0

Discrepancy between the mooring data and reanalyses can be partially explained by measurement data processing method. Unlike reanalyses, where there are no missing values, observational data are not continuous. The spatial averaging algorithms used can make a significant contribution to the simulated field quality. The ordinary kriging used in the present study showed satisfactory results. Kriging is sensitive to linearly arranged data as well as duplicate data. It should be noted that the problem of extrapolation is also acute in mooring data processing. Often the first horizon is below 50 m and the last one does not reach the bottom. To calculate integral transports, we are forced to use a fixed layer (in this study, the entire water column). For this purpose, the first measurement horizon is extrapolated to the surface. Bottom horizons are modelled using interpolation (if there are other observations in the area). Another factor explaining discrepancies in heat and mass transport estimates may be an insufficiently accurate assessment of recirculating waters in the Fram Strait in reanalysis data.

Heat and mass transport in the core of the Atlantic waters

A comparative analysis of series of heat and mass transport values in the AW core (temperature above 2 °C) was carried out to estimate the influence of shortcomings of the instrumental observation data and reanalysis products listed in the previous subsection on the result of comparison of heat and mass transport processes [10, 21]. It permitted to exclude data extrapolation, improve spatial interpolation quality, and avoid AW recirculation branches in the Fram Strait. In addition, the heat and mass transport estimate in the AW core is of fundamental scientific interest [11]. The methodology for calculating the integral transport of volume, heat and mass was like that described above for the entire Fram Strait. The calculation results are presented in Table 3.

T a b l e 3

Basic statistical characteristics of the studied monthly series of data for the Atlantic Ocean waters

Parameter	GLOR	ORAS	FOAM	CGLO	Ensemble	Mooring
			Fw			
Minimum	0.00	0.00	0.00	0.00	0.00	0.00
Maximum	2.44	2.58	3.20	2.87	2.52	3.59
Average	1.02	0.78	1.39	1.25	1.11	1.47
Standard deviation	0.60	0.52	0.61	0.52	0.45	0.64
Dispersion	0.36	0.27	0.37	0.27	0.20	0.41
			Fh			
Minimum	0.0	0.0	0.0	0.0	0.0	0.0
Maximum	54.0	47.0	69.0	60.0	55.0	87.0
Average	21.0	15.0	29.0	26.0	23.0	32.0
Standard deviation	13.0	11.0	13.0	11.0	10.0	15.0
Dispersion	169.0	121.0	169.0	121.0	100.0	225.0
			Fs			
Minimum	0.0	0.0	0.0	0.0	0.0	0.0
Maximum	89.0	94.0	117.0	105.0	92.0	130.0
Average	37.0	28.0	51.0	46.0	40.0	53.0
Standard deviation	22.0	19.0	22.0	19.0	16.0	23.0
Dispersion	484.0	361.0	484.0	361.0	256.0	529.0

Figure 7 shows that the heat and mass transport values within the Atlantic waters have significantly better consistency. The mooring data still show overestimations, but the residual does not exceed 25% of the ensemble mean. It is noteworthy that some reanalyses turned out to be much closer to the mooring data. Thus, the FOAM reanalysis underestimates the average values by only 6% and CGLO by 15%. The correlation analysis demonstrated that the ensemble of reanalyses shows the best agreement with observational data (Table 4).

If we talk about a separate model, then FOAM most closely describes the field data. Analysis of seasonal data showed that in the summer season reanalyses still significantly underestimate heat and mass transport in the Atlantic waters. The better consistency is observed in winter.

Table 4

Correlation coefficients between monthly averaged mooring data and reanalyses

Transport	GLOR	ORAS	FOAM	CGLO	Ensemble
F_w	0.37	0.46	0.52	0.50	0.59
F_h	0.47	0.53	0.55	0.51	0.62
F_s	0.37	0.46	0.52	0.50	0.59

Considering better consistency of the results for the AW core, equations of linear regression were constructed relating the heat and mass transport values calculated from instrumental observations and reanalysis products for the AW core (Fig. 8).

The time series of heat and mass transport through the Fram Strait based on the average monthly, seasonal, and annual data for the Atlantic waters are presented in Figs. 9–12.

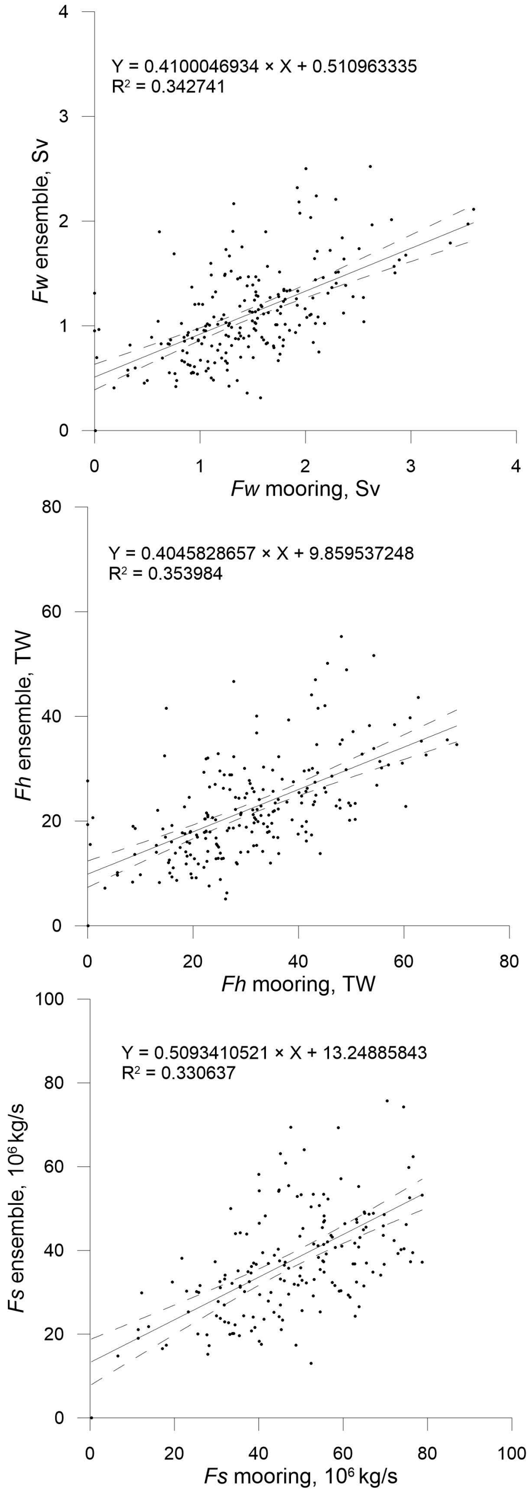

F i g. 8. Equations of linear regression between mooring data and model ensemble

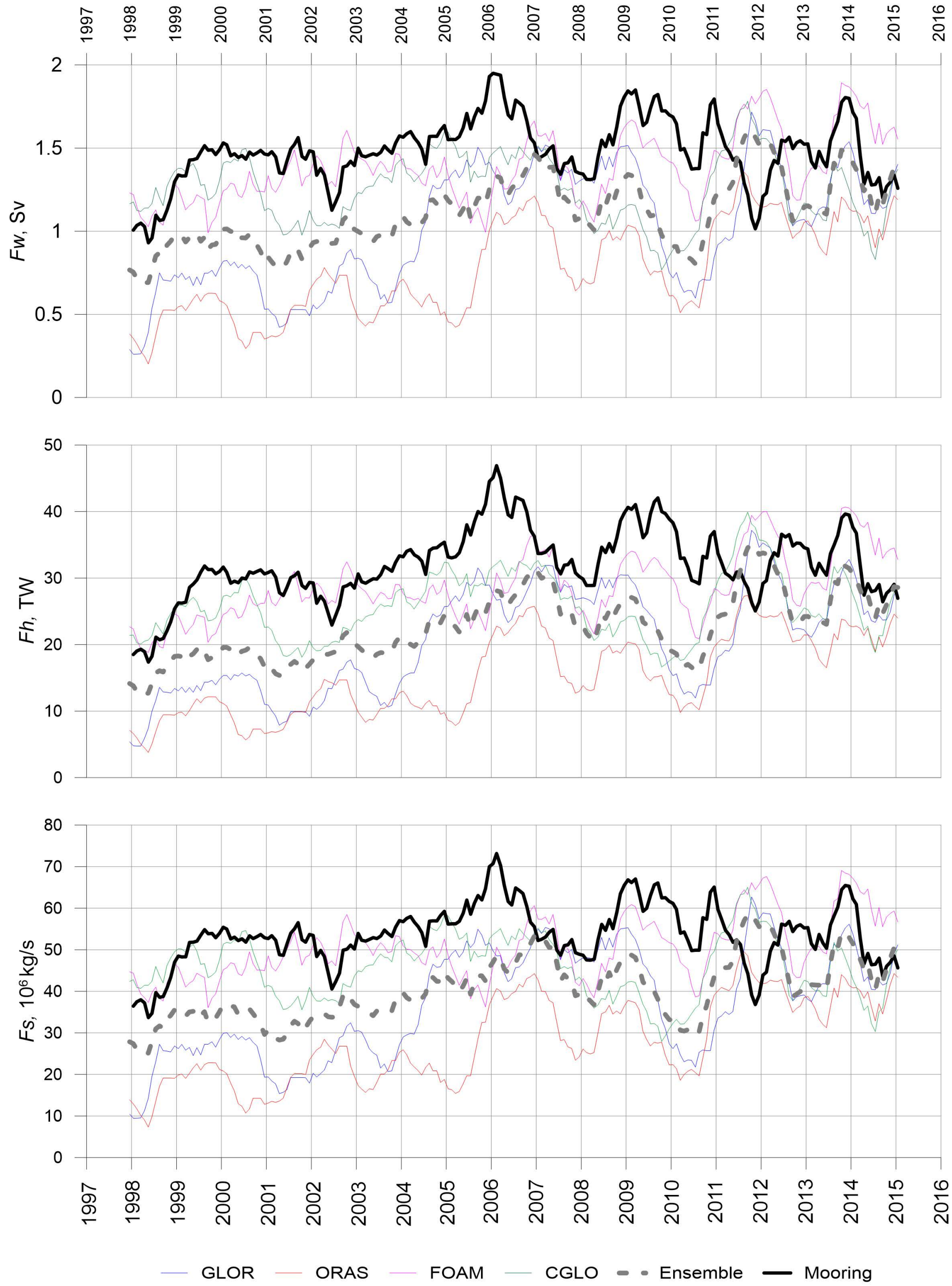

F i g. 9. Time series of heat and mass transport through the Fram Strait calculated by monthly average data for the Atlantic Ocean waters

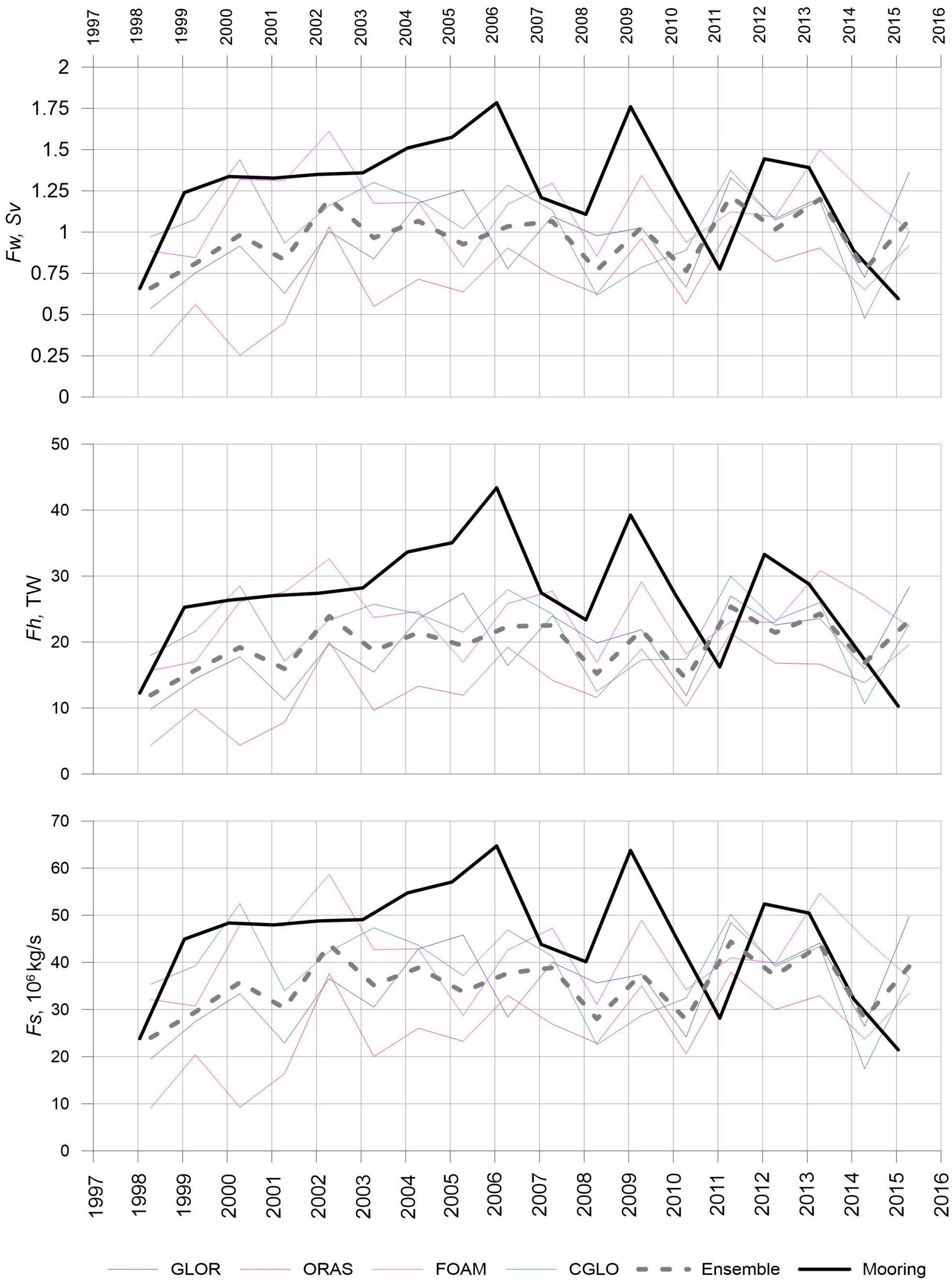

F i g. 10. Time series of heat and mass transport through the Fram Strait over summer season (April – September) for the Atlantic Ocean waters

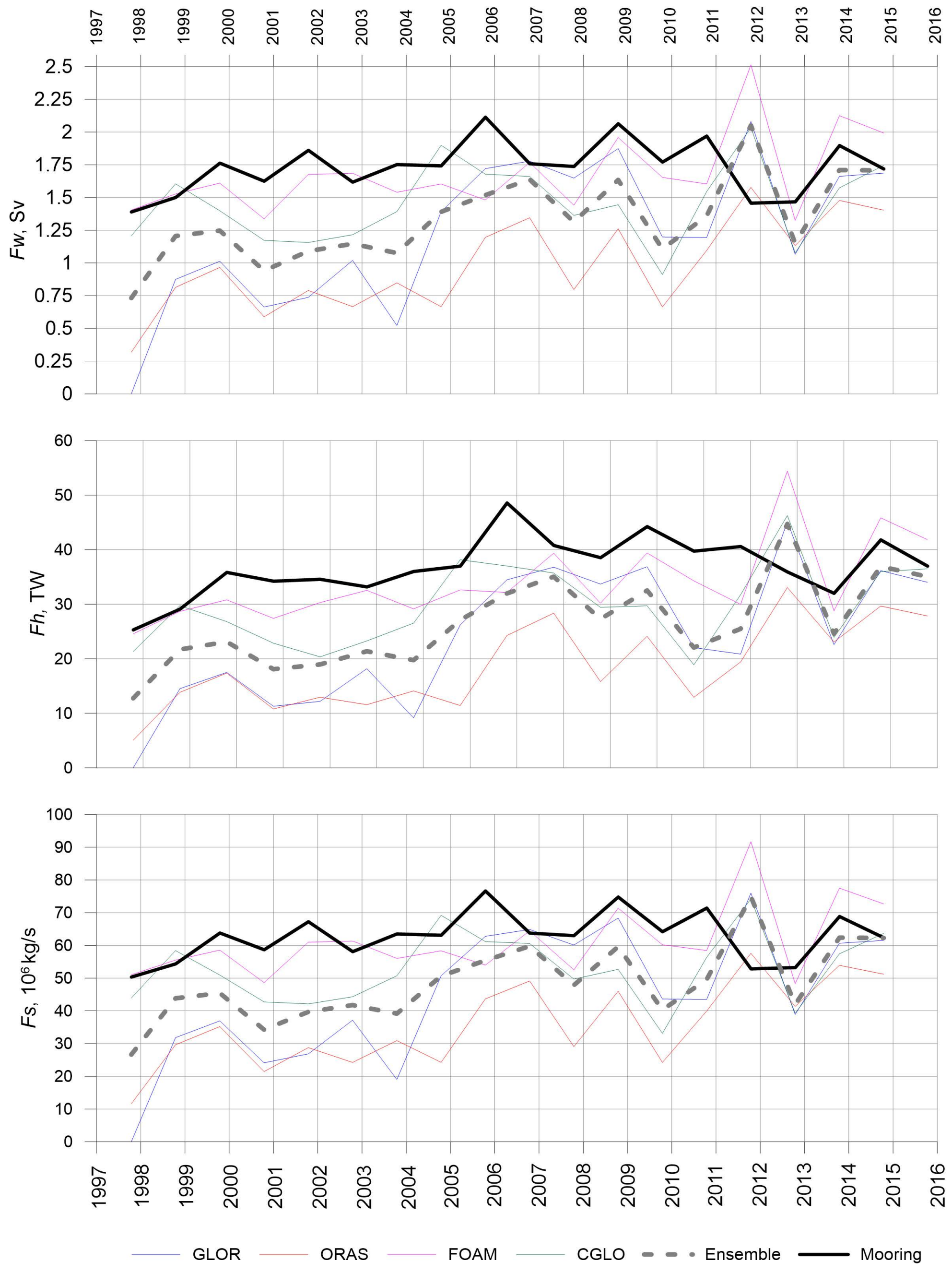

F i g. 11. Time series of heat and mass transport through the Fram Strait over winter season (October – March) for the Atlantic Ocean waters

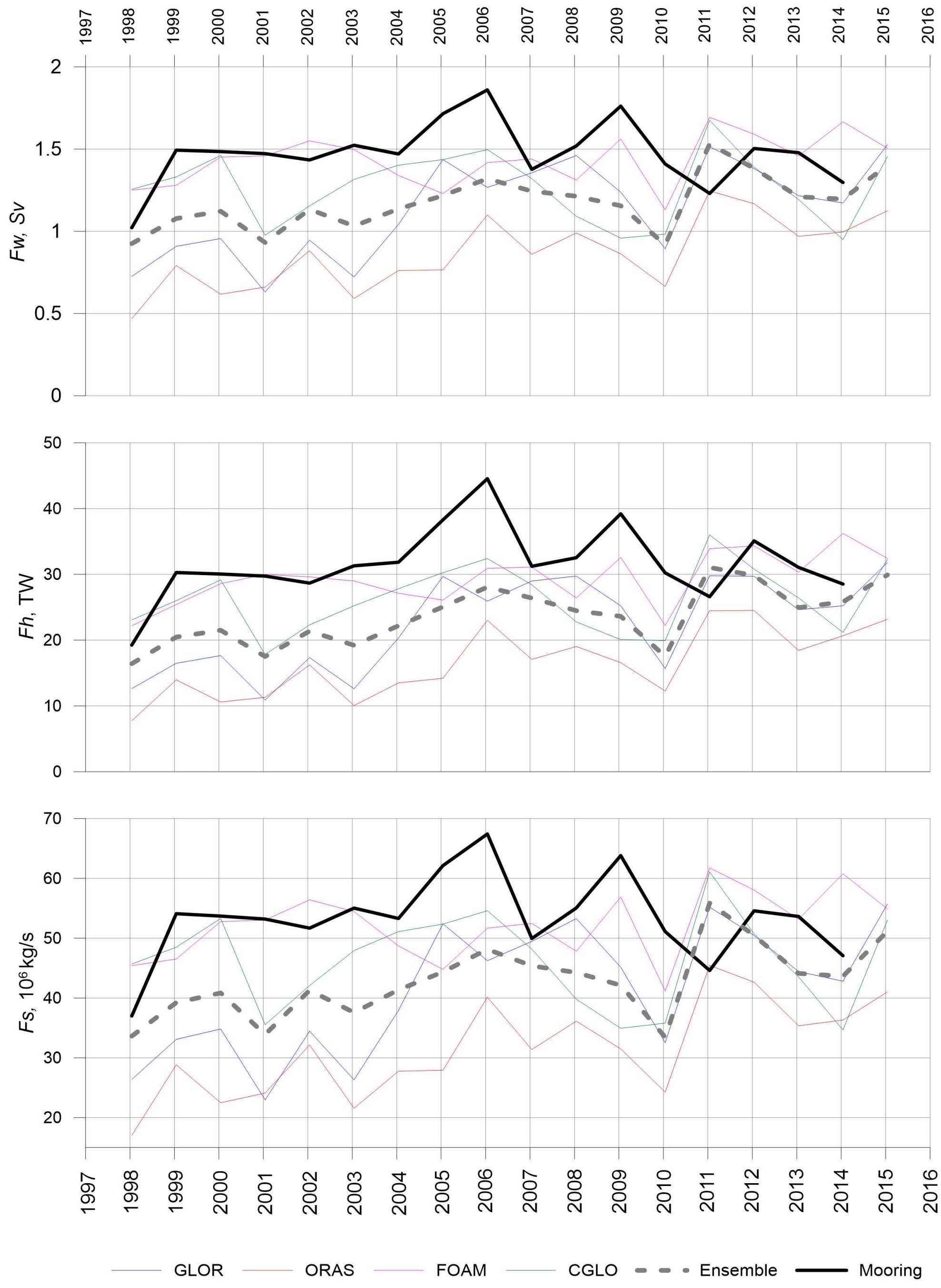

F i g. 12. Annual time series of heat and mass transport through the Fram Strait for the Atlantic Ocean waters

Conclusions

In the present paper, a comparative analysis of heat and mass transport processes in the Fram Strait, calculated from field observations (AWI and NPI moorings) and GLOR, ORAS, FOAM and CGLO reanalyses, was carried out. The mooring data were interpolated to regular grid points using ordinary kriging (6.5°W – 8°E, 25 m vertical).

Monthly data comparison showed that reanalyses generally underestimate volume, heat and salt transports by 30%. This may be due to both the shortcomings of spatial interpolation methods and the fact that the models do not accurately estimate recirculation waters.

Additional analysis of heat and mass transport processes associated with Atlantic waters (T > 2 °C) showed significantly better results. It is revealed that the ensemble of models describes observation data variability the best. Talking about individual products, preference is given to the FOAM and CGLO reanalyses describing most of the mooring temporal variability.

The data consistency in the winter period (October–March) is shown to be higher than that in the summer period (April–September). It can be related to reanalysis imperfections (counting ice melt) and the season, namely summer, when moorings are usually replaced, which can result in additional errors in combining time series.

REFERENCES

1. Ribal, A. and Young, I.R., 2019. 33 Years of Globally Calibrated Wave Height and Wind Speed Data Based on Altimeter Observations. *Scientific Data*, 6(1), 77. https://doi.org/10.1038/s41597-019-0083-9
2. Ribal, A. and Young, I.R., 2020. Calibration and Cross Validation of Global Ocean Wind Speed Based on Scatterometer Observations. *Journal of Atmospheric and Oceanic Technology*, 37(2), pp. 279-297. https://doi.org/10.1175/JTECH-D-19-0119.1
3. Levitus, S., Antonov, J.I., Boyer, T.P., Baranova, O.K., Garcia, H.E., Locarnini, R.A., Mishonov, A.V., Reagan, J.R., Seidov, D. [et al.], 2012. World Ocean Heat Content and Thermosteric Sea Level Change (0–2000 m), 1955-2010. *Geophysical Research Letters*, 39(10), L10603. https://doi.org/10.1029/2012GL051106
4. Lellouche, J.-M., Le Galloudec, O., Drévillon, M., Régnier, C., Greiner, E., Garric, G., Ferry, N., Desportes, C., Testut, C.-E., Bricaud, C. [et al.], 2013. Evaluation of Global Monitoring and Forecasting Systems at Mercator Océan. *Ocean Science*, 9(1), pp. 57-81. https://doi.org/10.5194/os-9-57-2013
5. Lellouche, J.-M., Greiner, E., Le Galloudec, O., Garric, G., Regnier, C., Drevillon, M., Benkiran, M., Testut, C.-E., Bourdalle-Badie, R. [et al.], 2018. Recent Updates to the Copernicus Marine Service Global Ocean Monitoring and Forecasting Real-Time 1/12° High-Resolution System. *Ocean Science*, 14(5), pp. 1093–1126. https://doi.org/10.5194/os-14-1093-2018
6. Blindheim, J. and Østerhus, S., 2005. The Nordic Seas, Main Oceanographic Features. In: H. Drange, T. Dokken, T. Furevik, R. Gerdes and W. Berger, eds., 2005. The *Nordic Seas: An Integrated Perspective*. Washington, D.C.: American Geophysical Union, pp. 11-37. https://doi.org/10.1029/158GM03
7. Timofeev, V.T., 1960. *Water Masses of the Arctic Basin*. Leningrad: Hydrometeoizdat, 191 p. (in Russian).
8. Polyakov, I.V., Alexeev, V.A., Bhatt, U.S., Polyakova, E.I. and Zhang, X., 2010. North Atlantic Warming: Patterns of Long-Term Trend and Multidecadal Variability. *Climate Dynamics*, 34(2-3), pp. 439-457. https://doi.org/10.1007/s00382-008-0522-3

9. Maslowski, W., Marble, D., Walczowski, W., Schauer, U., Clement, J.L. and Semtner, A.J., 2004. On Climatological Mass, Heat, and Salt Transports through the Barents Sea and Fram Strait from a Pan-Arctic Coupled Ice-Ocean Model Simulation. *Journal of Geophysical Research: Oceans*, 1099(C3), C03032. https://doi.org/10.1029/2001JC001039

10. Schauer, U., Fahrbach, E., Osterhus, S. and Rohardt, G., 2004. Arctic Warming through the Fram Strait: Oceanic Heat Transport from 3 Years of Measurements. *Journal of Geophysical Research: Oceans*, 109(C6), C06026. https://doi.org/10.1029/2003JC001823

11. Beszczynska-Möller, A., Fahrbach, E., Schauer, U. and Hansen, E., 2012. Variability in Atlantic Water Temperature and Transport at the Entrance to the Arctic Ocean, 1997–2010. *ICES Journal of Marine Science*, 69(5), pp. 852-863. https://doi.org/10.1093/icesjms/fss056

12. Ivanov, V.V., 2002. Atlantic Waters in the Western Arctic. In: A. P. Lisitsyn, M. E. Vinogradov and E. A. Romankevich, eds., 2002. *Integrated Oceanographic Studies in the Arctic Ocean*. Moscow: Nauchniy Mir, pp. 76-91 (in Russian).

13. Aagaard, K., Coachman, L.K. and Carmack, E., 1981. On the Halocline of the Arctic Ocean. *Deep Sea Research Part A. Oceanographic Research Paper*s, 28(6), pp. 529-545. https://doi.org/10.1016/0198-0149(81)90115-1

14. Wood, K.R., Jayne, S.R., Mordy, C.W., Bond, N., Overland, J.E., Ladd, C., Stabeno, P.J., Ekholm, A.K., Robbins, P.E. [et al.], 2018. Results of the First Arctic Heat Open Science Experiment. *Bulletin of the American Meteorological Society*, 99(3), pp. 513-520. https://doi.org/10.1175/BAMS-D-16-0323.1

15. Carton, J.A., Penny, S.G. and Kalnay, E., 2019. Temperature and Salinity Variability in the SODA3, ECCO4r3, and ORAS5 Ocean Reanalyses, 1993–2015. *Journal of Climate*, 32(8), pp. 2277-2293. https://doi.org/10.1175/JCLI-D-18-0605.1

16. Janout, M.A., Hölemann, J., Laukert, G., Smirnov, A., Krumpen, T., Bauch, D. and Timokhov, L., 2020. On the Variability of Stratification in the Freshwater-Influenced Laptev Sea Region. *Frontiers in Marine Science*, 7, 543489. https://doi.org/10.3389/fmars.2020.543489

17. Fahrbach, E., Meincke, J., Østerhus, S., Rohardt, G., Schauer, U., Tverberg, V. and Verduin, J., 2001. Direct Measurements of Volume Transports through Fram Strait. *Polar Research*, 20(2), pp. 217-224. https://doi.org/10.3402/polar.v20i2.6520

18. Lellouche, J.-M., Le Galloudec, O., Drévillon, M., Régnier, C., Greiner, E., Garric, G., Ferry, N., Desportes, C., Testut, C.-E. [et al.], 2013. Evaluation of Global Monitoring and Forecasting Systems at Mercator Océan. *Ocean Science*, 9(1), pp. 57-81. https://doi.org/10.5194/os-9-57-2013

19. Wackernagel, H., 1995. Ordinary Kriging. In: H. Wackernagel, 1995. *Multivariate Geostatistics: An Introduction with Applications*. Berlin, Heidelberg: Springer, pp. 74-81. https://doi.org/10.1007/978-3-662-03098-1_11

20. Korablyev, A.A. Pnyushkov, A.V. and Smirnov, A.V., 2008. Technology of Compiling Oceanographic Databases: A Case Study of the Arctic North European Basin. *Proceedings of the Russian State Hydrometeorological University*, (1), pp. 89-108 (in Russian).

21. De Steur, L., Hansen, E., Mauritzen, C., Beszczynska-Möller, A. and Fahrbach, E., 2014. Impact of Recirculation on the East Greenland Current in Fram Strait: Results from Moored Current Meter Measurements between 1997 and 2009. *Deep Sea Research Part I: Oceanographic Research Papers*, 92, pp. 26-40. https://doi.org/10.1016/j.dsr.2014.05.018

About the authors:

Aleksandr V. Smirnov, Senior Researcher, Arctic and Antarctic Research Institute (38 Bering Str., Saint Petersburg, 199397, Russian Federation), **ResearcherID: J-5935-2014, ORCID ID: 0000-0003-3231-7283**, **Scopus Author ID: 56264603400**, avsmir@aari.ru

Vladimir V. Ivanov, Chief Researcher, M.V. Lomonosov Moscow State University (1 Leninskie Gory, Moscow, 119991, Russian Federation), Arctic and Antarctic Research Institute (38 Bering Str., Saint Petersburg, 199397, Russian Federation)

Andrey A. Sokolov, Leading Engineer, Ice Hydrometeorological Information Center, Arctic and Antarctic Research Institute (38 Bering Str., Saint Petersburg, 199397, Russian Federation)

Contribution of the co-authors:

Aleksandr V. Smirnov – data preparation and analysis, numerical calculations, analysis and interpretation of the results, discussion and graphical representation of the results

Vladimir V. Ivanov – formulation of the research problem, analysis and interpretation of the results obtained in the study, discussion of the work results, formulation of conclusions

Andrey A. Sokolov – statistical data analysis, graphical presentation of the results

The authors have read and approved the final manuscript.
The authors declare that they have no conflict of interest.